

**Effect of Mesenchymal Stem Cell-Derived Microvesicles, Zinc Oxide Nanoparticles, and Advanced Platelet-Rich Fibrin on Tendon Healing in A Rabbit Model: Ultrasonographic and Locomotive Advancement Studies**

Mahmoud A. Hassan<sup>1</sup>, Mohamed W. El-Sherif<sup>1</sup>, Mohamed S. Abdelhakm<sup>1</sup>, Waleed Senosy<sup>2</sup>, Mahmoud T. Nassef<sup>3</sup>, Mohamed Abd Elkawi<sup>1\*</sup>

(1) Department of Surgery, Faculty of Veterinary Medicine, New Valley University, El-Kharga, 27511 New Valley, Egypt.

(2) Department of Theriogenology, Faculty of Veterinary Medicine, New Valley University, El-Kharga, 27511 New Valley, Egypt.

(3) Department of Surgery, Faculty of Veterinary Medicine, Assiut University, 27511 Assiut, Egypt.

\*Corresponding author: [mohamedabdelkawi@vet.nvu.edu.eg](mailto:mohamedabdelkawi@vet.nvu.edu.eg) Received: 20/10/2024  
accepted 29/11/2024.

**ABSTRACT**

Through the use of clinical locomotor and ultrasound measurements, this study was aimed at investigating the impact of advanced platelet-rich fibrin (A-PRF), mesenchymal stem cell-derived microvesicles (MVs), and zinc oxide nanoparticles (ZnO-NPs) on the healing of tendon defects in rabbits. Thirty-six adult male New Zealand rabbits were allocated into four equal groups. An Achilles tendon defect was induced. The control group was left untreated, A-PRF group treated with application of PRF membrane, ZnO-NP group was treated with 0.2% ZnO-NPs, and MV group treated with MSC-derived MVs. Healing was assessed through clinical and ultrasound evaluations at 2-, 4- and 6-weeks. Results revealed that all the treatment groups had better outcomes than the control group regarding lameness, pain during complete flexion of the tarsal joint, adhesion, and inflammation. The MVs and ZnO-NPs significantly decreased lameness and adhesion than the A-PRF and control groups. Ultrasonographic examination revealed a normal echogenic fibrillar pattern with normal margins and no evidence of ultrasonographic abnormalities in the MVs or ZnO-NP groups compared to other groups. Overall, ultrasonographic locomotive observation revealed the MVs and ZnO-NP groups' superiority in treating Achilles tendon defects compared with the A-PRF and control groups when used to fill a tendon defect in a rabbit model.

**Keywords:** Achilles tendon, Healing, Lameness, Zinc-oxide Nanoparticles, Microvesicles.

**INTRODUCTION**

Tendon injuries, particularly those affecting the Achilles tendon, pose substantial challenges in veterinary medicine. The tendon may deteriorate

as a result of several extrinsic causes, including steroids, medications, and fluoroquinolones. (SODE et al., 2007) as well as intrinsic factors such as age, sex, and obesity (HOLMES and LIN, 2006). Additionally, the self-repairing

ability of tendons is poor because resident cells are rare and their metabolism is high, which inhibits the repair process from being properly guided and restores native tissue function. (SHARMA and MAFFULLI, 2006; SHOJAEI and PARHAM, 2019). The Achilles tendon, which is crucial for locomotion and overall musculoskeletal integrity, often requires interventions that enhance its natural healing process (STEINMANN et al., 2020). Advanced platelet-rich fibrin (A-PRF) is one of platelet concentration materials and has many advantages in many of medicine fields (KARIMI and ROCKWELL, 2019). PRF can stimulate the healing process for a range of chronic tendons, bones, muscles, and other injuries of soft tissue (GRECU et al., 2019). It is a cytokine delivery vehicle that promotes cell viability, differentiation, proliferation and extracellular matrix synthesis (AL-HUSSEIN et al., 2023). Recently, mesenchymal stem cell-derived micro vesicles (MSCs-MVs) have been identified as a new therapeutic strategy for tissue regeneration (MOHAMMADI et al., 2020). Microvesicles (MVs), also known as microparticles, exosomes, and ectosomes, are membrane tiny vesicles that have the ability to transmit proteins, messenger RNA (mRNA), and microRNAs (miRNAs) into cells, causing changes in the recipient cells' gene expression, proliferation, and differentiation. (TSENG and HSU, 2014). Compared to MSCs, MVs not only play a pivotal role in regeneration and tissue repair but are also more durable and preservable (COCUCCI and MELDOLESI, 2015; PANT et al., 2012), inducing a greater protective effect that decreases over time. In addition, because of their small size, systemic administration of MVs

instead of MSCs may reduce safety concerns such as vascular occlusions (XIE et al., 2016). Numerous studies have examined the use of nanoparticles in textile materials with the goal of creating completed fabrics with various performance levels. For example, ZnO nanoparticles have been used for antibacterial properties (BECHERI et al., 2008), and have attracted increased amounts of research attention due to their safety (KHALIL et al., 2019; SINGH et al., 2021). ZnO-NPs are powerful wide-spectrum antibacterial agents with a tidal effect due to the generation of reactive oxygen species along with the rupture of the bacterial cell membrane (SINGH et al., 2021). Moreover, ZnO-NPs have been shown to enhance tendon, bone and soft tissue regeneration (EL-SHAER et al., 2022). Ultrasonography is a noninvasive, dynamic tool that provides real-time insights into tendon healing. Through ultrasonographic images, the echo pattern, width, depth, and cross-sectional area of the Achilles tendon can be measured, permitting us to obtain a nuanced understanding of regenerative processes over time, which will provide valuable data on the structural aspects of tendon healing (ALKETBI, 2016). This study addresses the regenerative potential of ZnO-NPs, A-PRF, and MVs in accelerating tendon healing using ultrasonographic assessments and lameness as key evaluation parameters.

## **MATERIALS AND METHODS**

### **Animals:**

The experimental protocol received approval from the Local Ethical Committee and the Institutional Review Board of the Faculty of Veterinary Medicine, New Valley University, in adherence to pertinent guidelines (ref. no. 4-2023-100086). Thirty-six adult male New Zealand

white rabbits, with an average weight of 2.5-3.5 kg, were utilized. The animals were housed singly in stainless steel cages under a controlled environment (25±5°C, 60-70% relative humidity, 12-hour light/dark cycle), access to dry food pellets and tap water, and a two-week acclimation period. All the rabbits were examined, and they were free of any musculoskeletal disorders.

### **Study Design:**

Animals were categorized into four groups: the control (untreated), A-PRF-treated, MV-treated, and ZnO-NP-treated groups. The control group was used to assess natural Achilles tendon healing, while the treated groups were treated with A-PRF membranes, MV gel, or ZnO-NP solution.

### **Preparation and Application of Interventions:**

Advanced Platelet-Rich Fibrin (A-PRF): Prepared following *Abd-Elkawi et al.'s* protocol (ABD-ELKAWI et al., 2023), A-PRF membranes were applied around the tendon defect.

MVs: MVs gel, derived from lyophilized MSC extracellular vesicles (EL-TOOKHY et al., 2017), was injected around the tendon defect in the MV-treated group.

ZnO-NPs: A 0.2% ZnO-NP (ZALAMA et al., 2022) solution was injected around the tendon defect in the ZnO-NP treatment group.

### **Surgical procedure:**

An incision of one cm, gently curved, was made laterally to the Achilles tendon. Following the creation of the skin flap, two parallel incisions, each 0.5 mm wide and 5 mm long, were

made in the Achilles tendon. These incisions extended from the tendon-bone insertion at the calcaneus to the mid-tendon, ensuring a full-thickness defect in the mid-substance of the tendon. (Figure 1). Once the tendon defect was established, the respective biomaterials were applied to the treatment groups as follows:

- *Control Group:* No biomaterial was applied, allowing for the natural healing process to occur.
- *A-PRF Treatment Group:* Advanced PRF membranes were carefully placed between and around tendon defect.
- For the MV-treated group, MV gel was injected between and around the tendon defect, and this process was repeated twice within a two-week interval.
- *ZnO-NP Treatment Group:* A 0.2% ZnO-NP solution, prepared as previously described, was injected around the tendon defect.

Study design, animal grouping and treatment administration are illustrated in Figure 2.

Following the application of biomaterials, meticulous closure of the subcutaneous tissues and skin was performed using standard surgical techniques. Post closure of the skin, a splint cast was used to immobilize the operative limb for a week., ensuring minimal disturbance to the applied biomaterials and facilitating a controlled healing environment. Throughout the entire procedure, efforts were made to minimize variability, providing a consistent and reproducible model for subsequent evaluations.

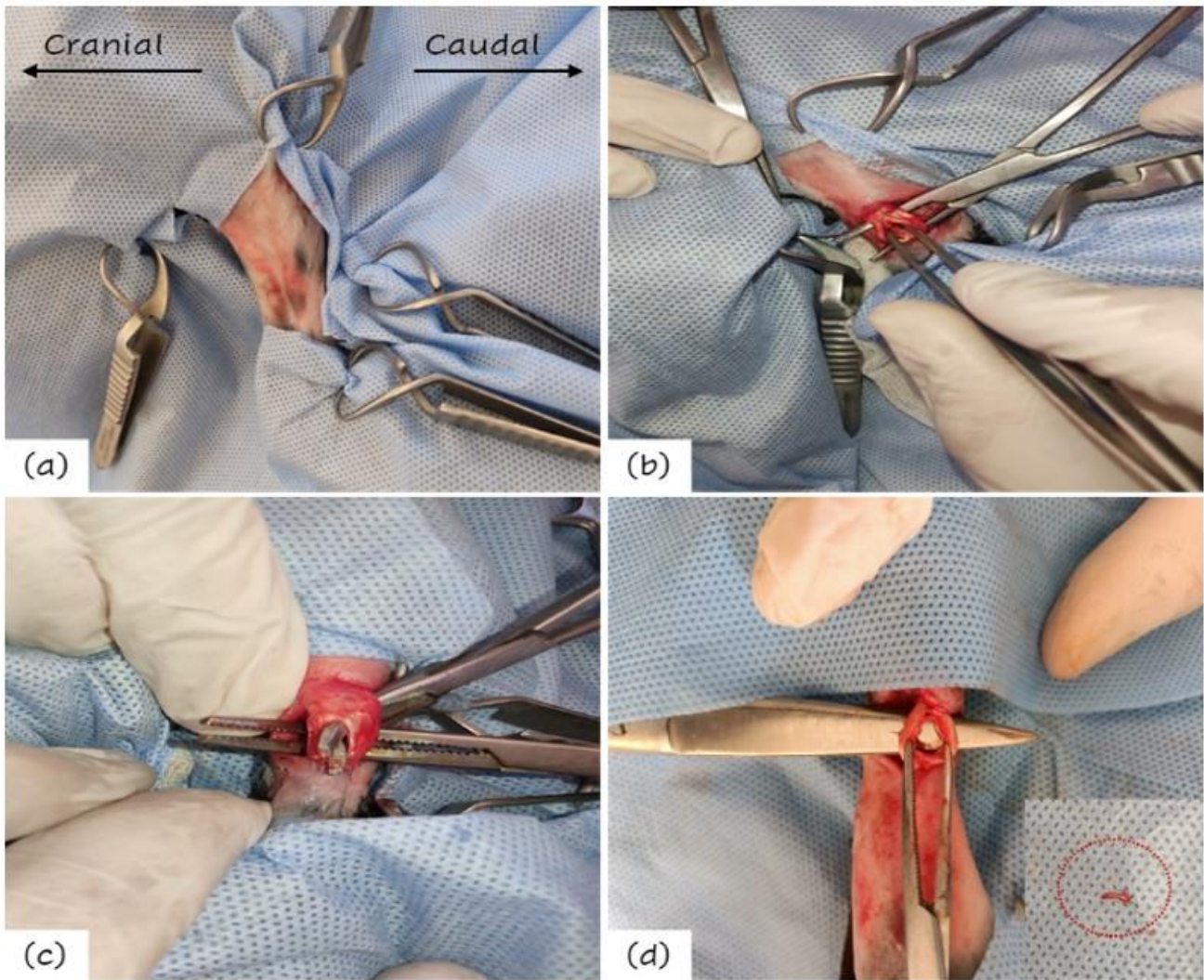


**Figure 1.** Induction of a split tendon rabbit model. The surgical procedure encompasses preparation of the surgical site (a), exposure of the Achilles tendon, splitting of the tendon (c), and removal of a central tendon strip (d).

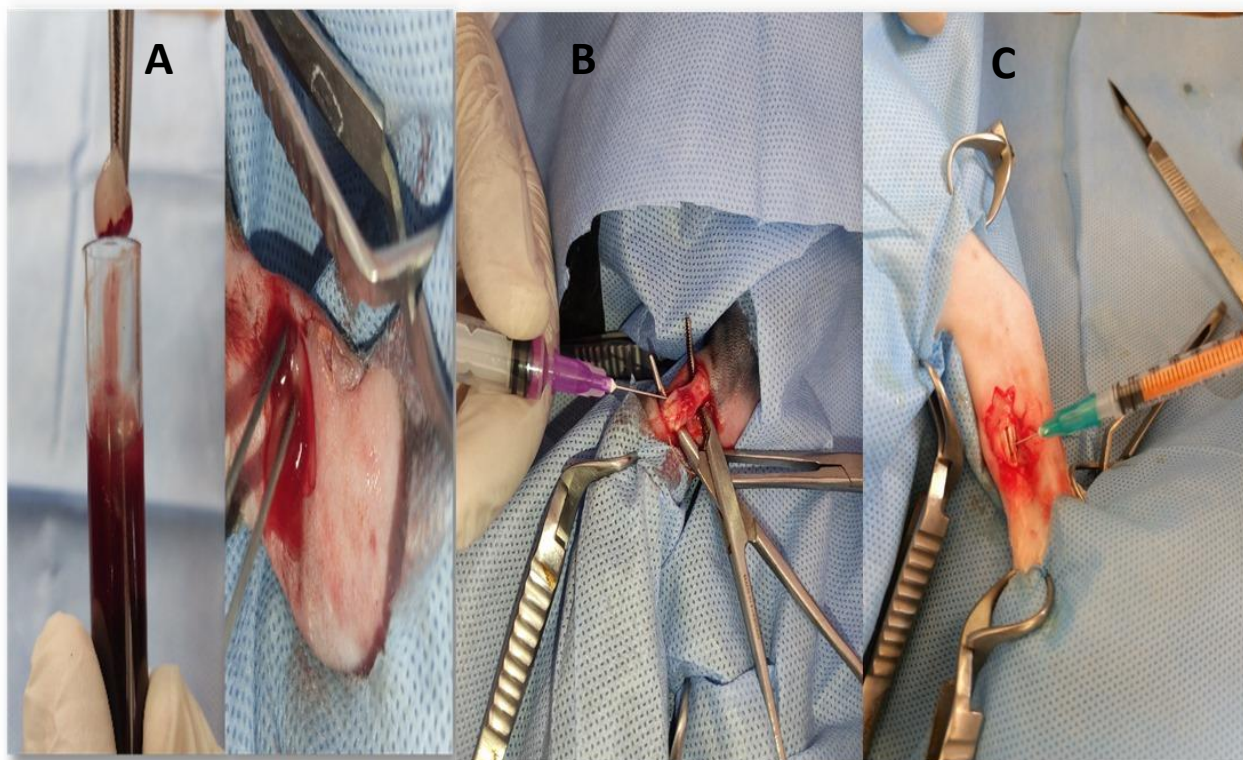


**Figure 2.** Application of biomaterials into Achilles tendon defect. A. (A.PRF) membrane into Achilles tendon defect, B. (MVs) injection into and around Achilles tendon defect and C. (ZnO-NPs) injection into and around Achilles tendon defect.

**Post-operative follow-up evaluation:**

Following their procedure, the rabbits were kept in a warm room at 37°C until they were completely awake. Upon regaining consciousness, the rabbits were carefully transferred to their individual cages. The rabbits were closely monitored for any signs of distress, general health, feeding, weight, temperature, or breathing. Wound healing and movement were observed. A dose of 0.6 mg/kg of meloxicam (Anticox II 15 mg, ADWIA, Egypt) was given to control postoperative pain.

**Clinical and locomotor evaluation:**

All the groups were subjected to clinical and lameness examinations based on the blind observer's reports, and the assessments were performed at the 2<sup>nd</sup>, 4<sup>th</sup> and 6<sup>th</sup> weeks post

implantation. Lameness and comfortable/uncomfortable physical activities were assessed both in the cage and on the floor. Pain upon palpation of the injured area and pain in complete or incomplete flexion of the tarsal joint were assessed through a numerical scale in which a score of zero was considered to indicate worsening or abnormal pain. This numerical scale was modified from those scales previously mentioned by (CONZEMIUS et al., 2002; KIM et al., 2010; STOLL et al., 2011).

**Ultrasonographic evaluation:**

Preoperative ultrasound in the longitudinal plane was performed. A numerical scoring system (Table 2) was used to evaluate tendon healing based on echo patterns according to *Saini et al.* (SAINI et al., 2010) Preoperative evaluations were

performed to establish baseline measurements and reference values using a Sonar device (Mindray DP-20, MSL, Guangdong China) equipped with a 10-14 MHz linear array probe.

Post implantation, ultrasonographic examinations were conducted at the 2<sup>nd</sup>, 4<sup>th</sup>, and 6<sup>th</sup> weeks post implantation. Longitudinal (LS) plane images were acquired with the U.S.

beam set at a depth of 2-3 cm and a gain of 50%. The LS images were analyzed for echo patterns and tendon fiber arrangement utilizing a numerical scoring system based on previously described criteria (Table 1). The ultrasonographic images of the individuals in the examined groups were assessed blindly by two specialists.

**Table 1:** Numerical scoring system for ultrasonographic evaluation of tendon healing according to Saini et al. (SAINI et al., 2010).

Score	Description
1	assigned when most of the area (80%) was anechoic.
2	assigned when half the area was anechoic, and half was a hypo echoic.
3	indicated that most of the area (80%) was hypo echoic.
4	Indicated the normal echotexture of the tendon, i.e., mottled hypo-echoic to hyperechoic texture.

#### **Histopathological examination:**

Six weeks following the operation, the Achilles tendons were removed by dissection at the calcaneal insertion and just below the musculo-tendinous junction. The extracted tendons underwent physiological buffer washing, 48 hours of fixing in 10% buffered formalin, dehydration, xylene clearing, and paraffin embedding. Haematoxylin and eosin (H&E) were used to stain thin longitudinal sections, 4-5 µm in thickness, that were cut from the paraffin blocks that had hardened.

#### **Statistical analysis:**

The results were analyzed as the median ± standard deviation. Statistical analyses were performed using one-way ANOVA. P-value ≤0.05 was considered a statistical significance. The statistical analysis was conducted using SPSS software (version 19.0; IBM, America).

## **RESULTS**

#### **Clinical and locomotor findings:**

Regarding the general health condition of the rabbits, all rabbits in the treated and control groups were in good health by the 2<sup>nd</sup> week post implantation. Moreover, statistical analysis revealed no significant differences at any of the evaluation times or among the groups. The total clinical and locomotor evaluation scores were significantly different at all time points (P= 0.00) among all the experimental groups (P=0.000-0.001) (Table 2) (Figure 3). Lameness was observed in all groups at 2 weeks post implantation but subsequently decreased gradually by 4 weeks post implantation and disappeared in the MVS- and ZnO-NP-treated groups at 6 weeks post implantation. During manipulation of the operated leg in the 2<sup>nd</sup> week of the experiment, every rabbit in the tested groups displayed evidence of discomfort; however, the control group had more obvious signals of pain than the other groups. Pain decreased

gradually until it disappeared at the 6<sup>th</sup> week post implantation. All of the animals showed evidence of complete flexion of the tarsal joint in the operated limbs by the 2<sup>nd</sup> week following implantation; however, this flexion was more pronounced in the control group than in the other treatment groups and subsequently decreased until it vanished in the A-PRF, MVS, and ZnO-NP groups at the 6<sup>th</sup> week. Tendon adhesion to the skin was observed at the 2<sup>nd</sup> week post

implantation in all groups, but it was more obvious in the control group than in other groups and then decreased gradually until the tendon became more slidable at the 6<sup>th</sup> week post implantation in the treated groups. Inflammation was present in all groups during the second postoperative week; it progressively subsided and vanished by the sixth postoperative week, except for the MVS- and ZnO-NP-treated groups.

**Table 2:** Results of clinical and locomotor score in control, A-PRF, MVS and ZnO-NP groups.

Groups	Times (weeks)			P value
	2w	4w	6w	
<b>General health condition of rabbit</b>				
Control	0 (0 - 0) <sup>*b</sup>	1 (0 - 1) <sup>*a</sup>	1 (1 - 1) <sup>a</sup>	<b>0.027</b>
A-PRF	0 (0 - 0) <sup>*</sup>	1 (1 - 1) <sup>*</sup>	1 (1 - 1)	-
MVS	0 (0 - 1) <sup>*b</sup>	1 (1 - 1) <sup>*a</sup>	1 (1 - 1) <sup>a</sup>	<b>0.079</b>
ZnO-NPs	0 (0 - 1) <sup>*b</sup>	1 (1 - 1) <sup>*a</sup>	1 (1 - 1) <sup>a</sup>	<b>0.079</b>
p. value	<b>0.596</b>	<b>0.441</b>	-	
<b>Lameness</b>				
Control	1 (0 - 1) <sup>*b</sup>	1 (1 - 2) <sup>*a</sup>	2 (2 - 2) <sup>*a</sup>	<b>0.031</b>
A-PRF	1 (1 - 1) <sup>*,**b</sup>	2 (2 - 2) <sup>*,***a</sup>	2 (2 - 3) <sup>*,***a</sup>	<b>0.007</b>
MVS	2 (1 - 3) <sup>**,**a</sup>	2 (2 - 3) <sup>**,**a</sup>	3 (2 - 3) <sup>*,**a</sup>	<b>0.579</b>
ZnO-NPs	2 (2 - 3) <sup>***a</sup>	3 (3 - 3) <sup>***a</sup>	3 (3 - 3) <sup>**a</sup>	<b>0.079</b>
p value	<b>0.039</b>	<b>0.007</b>	<b>0.077</b>	
<b>Pain on manipulation</b>				
Control	0 (0 - 0) <sup>*a</sup>	0 (0 - 1) <sup>*a</sup>	1 (0 - 1) <sup>*a</sup>	<b>0.296</b>
A-PRF	0 (0 - 0) <sup>*c</sup>	1 (1 - 1) <sup>*,**b</sup>	2 (1 - 2) <sup>**a</sup>	<b>0.003</b>
MVS	0 (0 - 1) <sup>*b</sup>	1 (1 - 2) <sup>**a</sup>	2 (2 - 2) <sup>***a</sup>	<b>0.014</b>
ZnO-NPs	1 (1 - 1) <sup>**a</sup>	2 (1 - 2) <sup>**a</sup>	2 (2 - 2) <sup>***a</sup>	<b>0.027</b>
p value	<b>0.009</b>	<b>0.055</b>	<b>0.002</b>	
<b>pain in complete flexion of the tarsal joint</b>				
Control	0 (0 - 0) <sup>*b</sup>	1 (0 - 1) <sup>*b</sup>	2 (1 - 2) <sup>*a</sup>	<b>0.014</b>
A-PRF	0 (0 - 1) <sup>*b</sup>	2 (2 - 2) <sup>**a</sup>	3 (2 - 3) <sup>**a</sup>	<b>0.002</b>
MVS	1 (1 - 1) <sup>**c</sup>	2 (2 - 2) <sup>**b</sup>	3 (2 - 3) <sup>**a</sup>	<b>0.003</b>

<b>ZnO-NPs</b>	0 (0 - 0) <sup>*c</sup>	2 (1 - 2) <sup>**b</sup>	3 (3 - 3) <sup>**a</sup>	<b>0.000</b>
<b>p value</b>	<b>0.009</b>	<b>0.012</b>	<b>0.052</b>	
<b>Connection of tendon to skin</b>				
<b>Control</b>	0 (0 - 0) <sup>*a</sup>	0 (0 - 0) <sup>*a</sup>	0 (0 - 1) <sup>*a</sup>	<b>0.422</b>
<b>A-PRF</b>	0 (0 - 0) <sup>*a</sup>	0 (0 - 1) <sup>*a</sup>	1 (0 - 1) <sup>*a</sup>	<b>0.296</b>
<b>MVS</b>	0 (0 - 1) <sup>*b</sup>	1 (1 - 1) <sup>**a</sup>	1 (1 - 1) <sup>*a</sup>	<b>0.079</b>
<b>ZnO-NPs</b>	1 (0 - 1) <sup>*a</sup>	1 (1 - 1) <sup>**a</sup>	1 (1 - 1) <sup>*a</sup>	<b>0.422</b>
<b>p value</b>	<b>0.219</b>	<b>0.006</b>	<b>0.596</b>	
<b>Inflammation</b>				
<b>Control</b>	0 (0 - 0) <sup>*</sup>	0 (0 - 0) <sup>*</sup>	1 (1 - 1) <sup>*</sup>	-
<b>A-PRF</b>	0 (0 - 0) <sup>*b</sup>	1 (1 - 1) <sup>**a</sup>	1 (1 - 2) <sup>*a</sup>	<b>0.007</b>
<b>MVS</b>	0 (0 - 1) <sup>*b</sup>	1 (1 - 2) <sup>**a</sup>	2 (2 - 2) <sup>**a</sup>	<b>0.014</b>
<b>ZnO-NPs</b>	0 (0 - 1) <sup>*b</sup>	2 (1 - 2) <sup>**a</sup>	2 (2 - 2) <sup>**a</sup>	<b>0.001</b>
<b>p value</b>	<b>0.596</b>	<b>0.005</b>	<b>0.006</b>	
<b>Total clinical and locomotor evaluation score</b>				
<b>Control</b>	2 (1 - 2) <sup>*b</sup>	3 (2 - 3) <sup>*b</sup>	7 (6 - 8) <sup>*a</sup>	<b>0.000</b>
<b>A-PRF</b>	1 (1 - 2) <sup>*c</sup>	7 (6 - 7) <sup>**b</sup>	9 (9 - 10) <sup>**a</sup>	<b>0.000</b>
<b>MVS</b>	3 (3 - 3) <sup>**c</sup>	9 (8 - 9) <sup>***b</sup>	11 (11 - 12) <sup>***a</sup>	<b>0.000</b>
<b>ZnO-NPs</b>	4 (3 - 4) <sup>**c</sup>	10 (10 - 11) <sup>****b</sup>	12 (11 - 12) <sup>***a</sup>	<b>0.000</b>
<b>p value</b>	<b>0.001</b>	<b>0.000</b>	<b>0.000</b>	

\* , \*\* , and \*\*\* : median and standard deviations with different asterisk superscripts in the same column are significantly different at P <0.05.

a, b, c: Means and standard deviations with different lowercase letters in the same row are significantly different at P <0.05.

### Total clinical and locomotor evaluation score

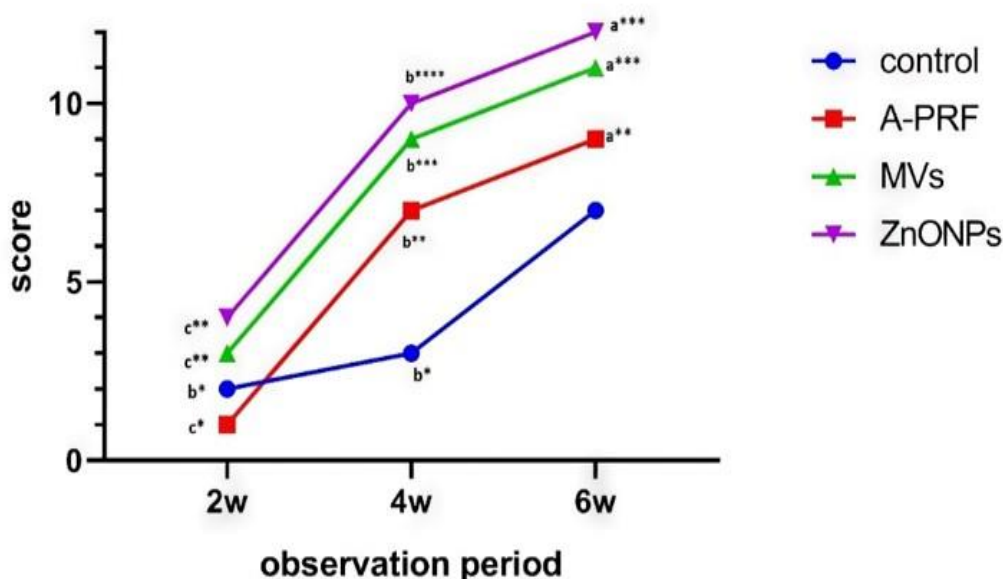


**Figure 3:** Total clinical and locomotor evaluation scores revealed significant differences among the four groups ( $P = 0.000-0.000$ ) at the 2nd, 4th, and 6th postoperative weeks ( $P = 0.000$ ). At the end of the observation period, there was no significant difference between the MV and ZnO-NP groups ( $P=0.058$ ), but there was a significant difference between the two groups and between the A-PRF and control groups.

#### Ultrasound findings (table 3) (fig: 8):

Ultrasonographic evaluation revealed significant differences among the four groups at the 4th and 6th postoperative weeks. At 2 weeks, there was no significant difference among the control, A-PRF and ZnO-NP groups, but there was a significant difference between the three groups and the MV group. At the end of the observation period (at six weeks), the highest ultrasonographic score was obtained in the MV and ZnO-NP groups ( $P= 4$ ). (table 3 - Fig. 8) In the control group, ultrasonography of the Achilles tendon at the 2<sup>nd</sup> week revealed the presence of an entangled hyperechoic area in the distal region (tendon insertion), loss of a normal fibrillar pattern, irregularity of tendon margins, and the presence of a hypoechoic area in the mid-section of the Achilles tendon. At the 4<sup>th</sup> week,

there were irregularities in the tendon margins and a loss of the normal fibrillar pattern. At the 6<sup>th</sup> week, there were irregularities in the tendon margins (Figure 4). In the A-PRF group, ultrasonographic examination at 2 weeks post implantation revealed a hyperechoic area, loss of the normal fibrillar pattern, and irregularity in the tendon margins. At 4 weeks post implantation, there was an irregular fibrillar pattern and hyperechoic area along the course of the tendon. Later, at 6 weeks post implantation, there were irregular tendon margins, hyperechoic areas along the tendon fibrils and irregular fibrillar patterns. (Fig. 5) Evaluation of ultrasonographic images of the MV and ZnO-NP groups revealed that 2 weeks post implantation, a hypoechoic area, an irregular fibrillar pattern and irregular tendon margins were present. At 4

weeks post implantation, ultrasonographic examination revealed only irregular tendon margins. At 6 weeks post implantation, ultrasonographic examination revealed

a normal echogenic fibrillar pattern with normal margins and no evidence of ultrasonographic abnormalities (Figs. 6, 7).

**Control untreated group:**

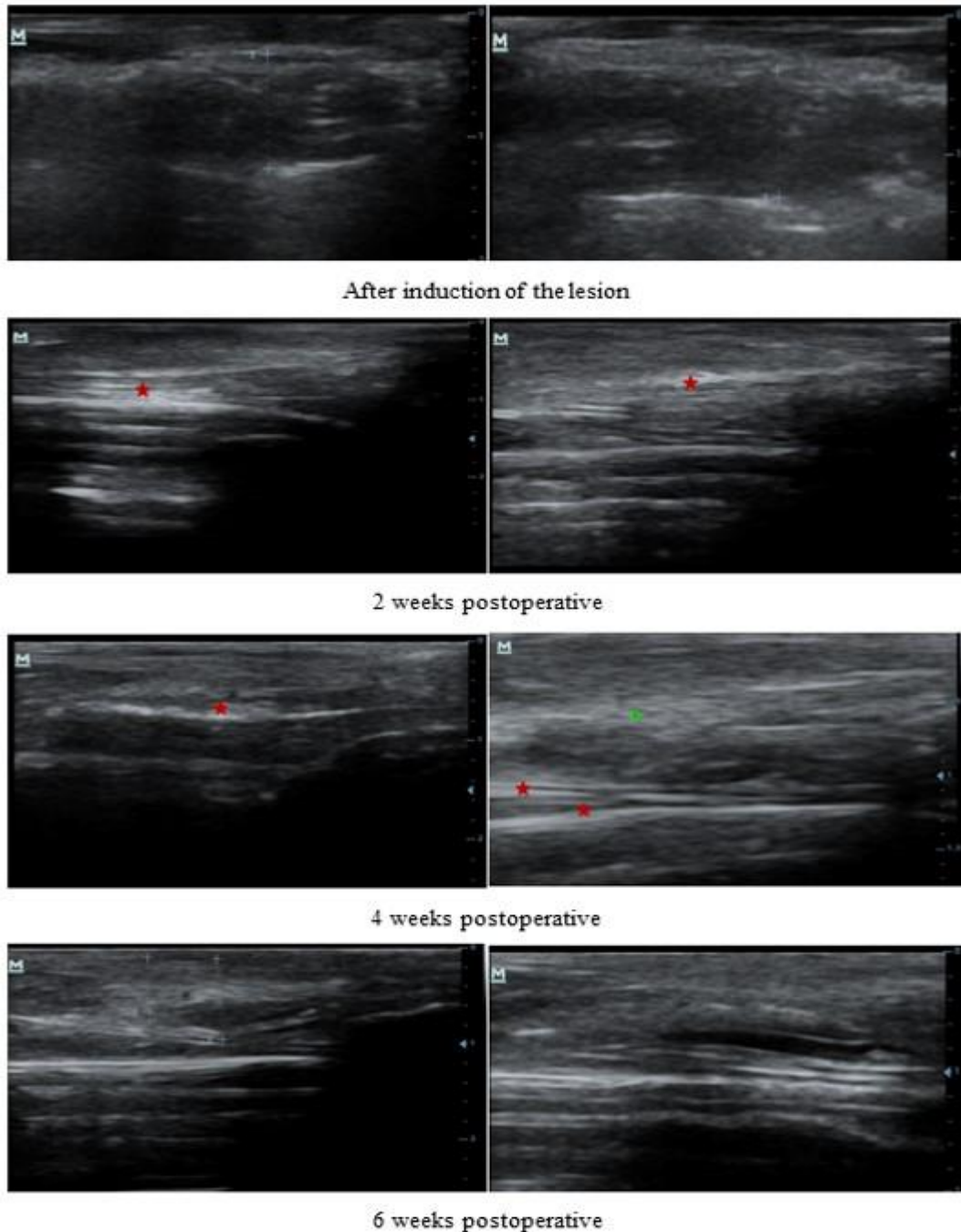


**Figure 4.** Ultrasonographic findings in the control untreated group at 0-, 2-, 4- and 6-weeks post-surgery. The red star indicates fibrous tissue formation, the orange star indicates edema and inflammatory exudate, and the green star indicates a normal arrangement of tendon fibers.

**A-PRF treatment group:**

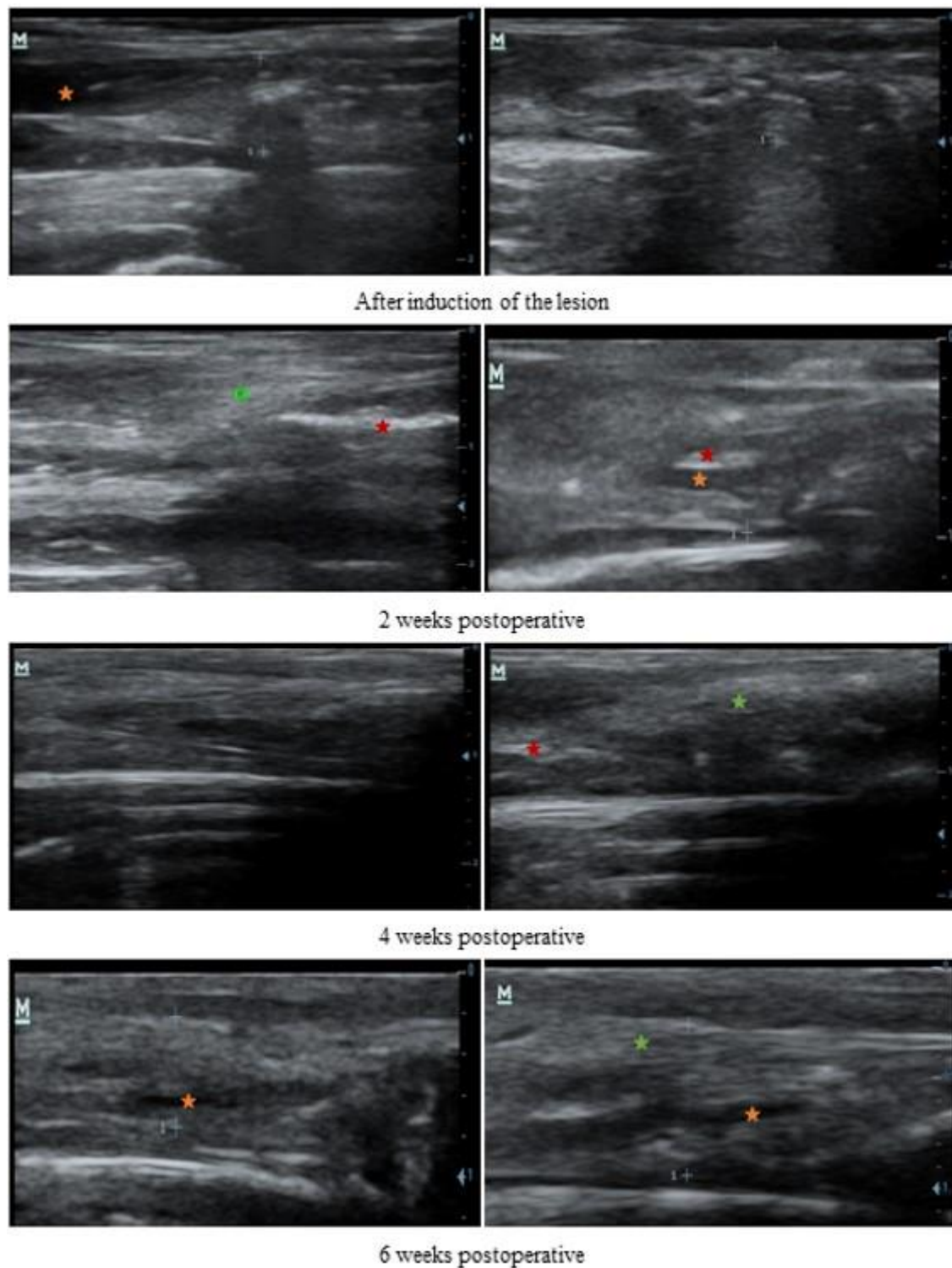


**Figure 5.** Ultrasonographic findings in the A-PRF-treated group at 0, 2, 4 and 6 weeks after surgery. The red star indicates fibrous tissue formation, the orange star indicates edema and inflammatory exudate, and the green star indicates a normal arrangement of tendon fibers.

**MV-treated group:**

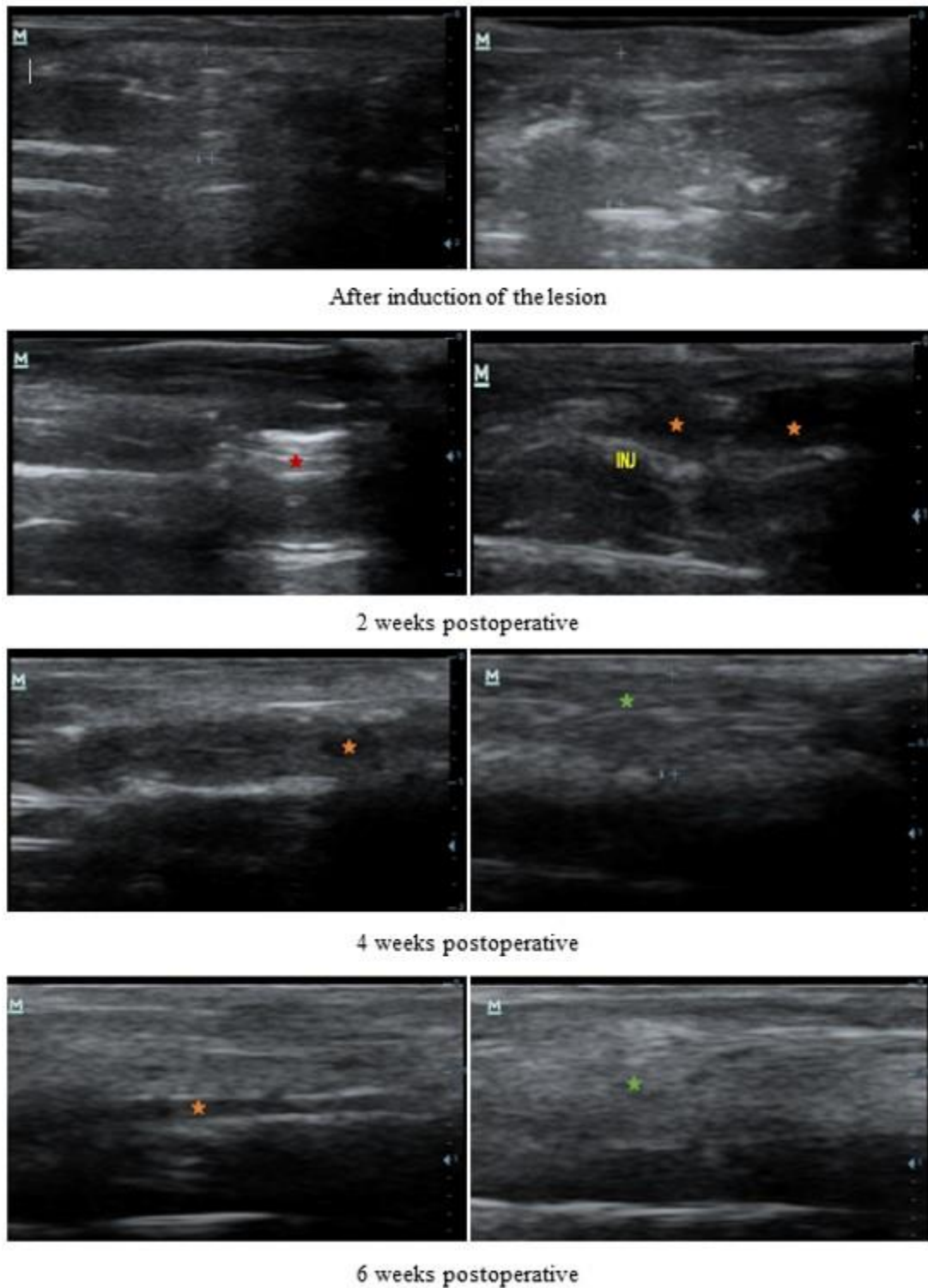


**Figure 6.** Ultrasonographic findings in the MV-treated group at 0, 2, 4 and 6 weeks after surgery. The red star indicates fibrous tissue formation, the orange star indicates edema and inflammatory exudate, and the green star indicates a normal arrangement of tendon fibers.

**ZnO-NP-treated group:**

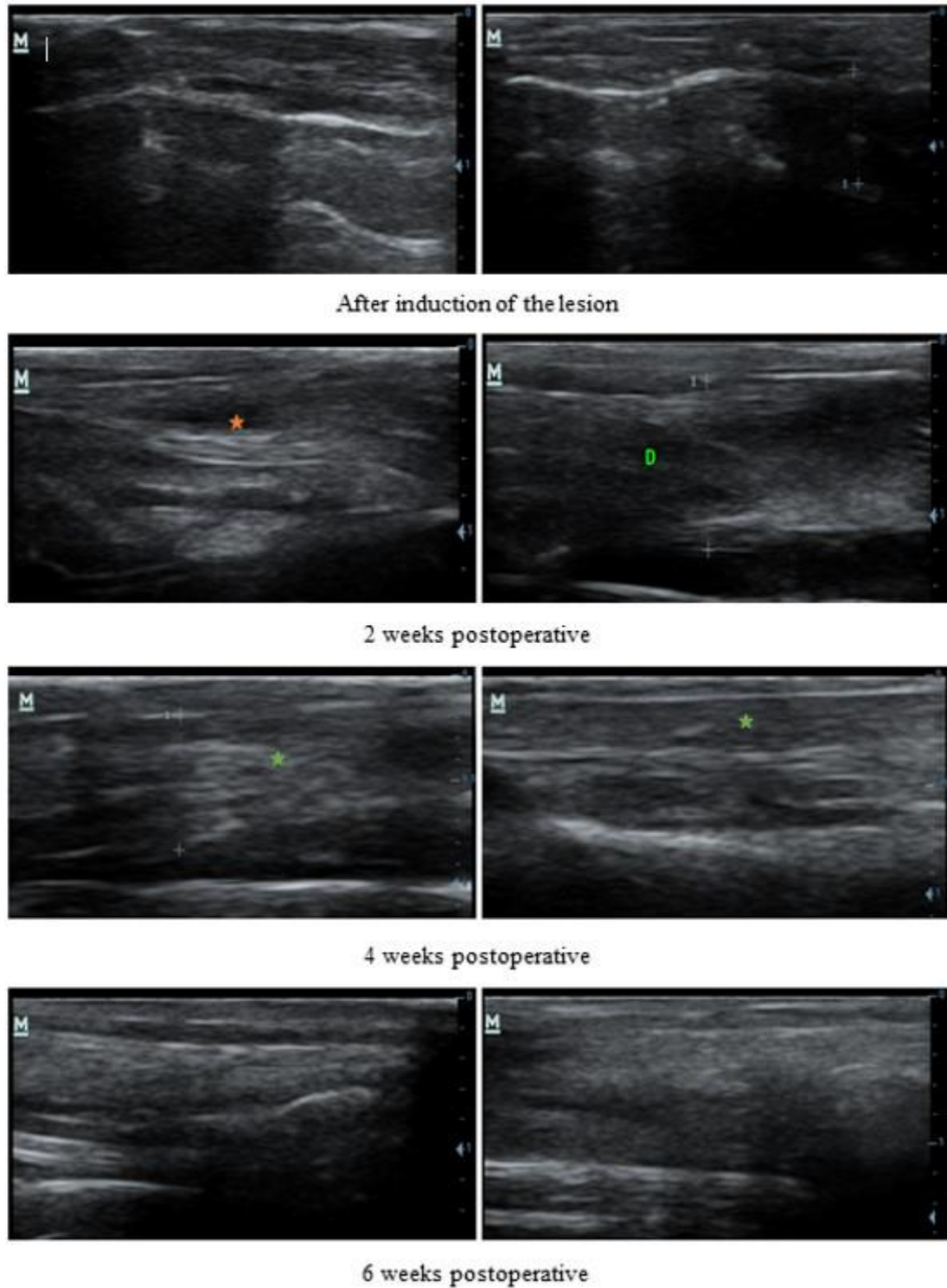


**Figure 7.** Ultrasonographic findings in the ZnO-NP-treated group at 0-, 2-, 4- and 6-weeks post-surgery. The red star indicates fibrous tissue formation, the orange star indicates edema and inflammatory exudate, and the green star indicates a normal arrangement of tendon fibers.

**Table 3:** Results of ultrasound score in the control, A-PRF, MVS and ZnO-NP groups.

Groups	Times ( weeks )			P-value
	2 w	4 w	6 w	
Control	1 (1 - 1) <sup>*b</sup>	1 (1 - 2) <sup>*b</sup>	2 (2 - 3) <sup>*a</sup>	<b>0.031</b>
A-PRF	2 (1 - 2) <sup>*,**b</sup>	2 (2 - 2) <sup>*,**ab</sup>	3 (2 - 3) <sup>*,**a</sup>	<b>0.098</b>
MVS	2 (2 - 2) <sup>**b</sup>	3 (2 - 3) <sup>**,***b</sup>	4 (3 - 4) <sup>**,***a</sup>	<b>0.014</b>
ZnO-NPs	2 (1 - 2) <sup>*,**b</sup>	3 (3 - 4) <sup>**,***a</sup>	4 (3 - 4) <sup>**,***a</sup>	<b>0.011</b>
p-value	<b>0.085</b>	<b>0.006</b>	<b>0.045</b>	

\*,\*\*,\*\*\* in the same column are significantly different at P < 0.05. a, b Median (minimum-maximum) values with different letters in the same row are significantly different at P<0.05.

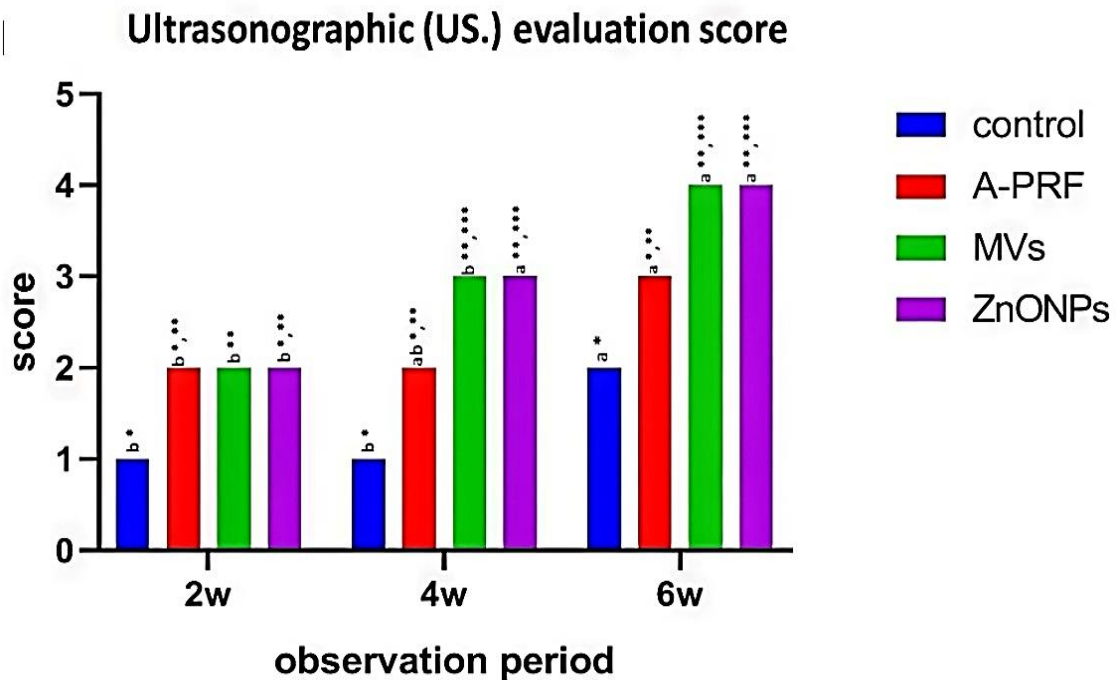


**Figure (8)** shows significant differences in ultrasonographic evaluation scores among the four groups at the 4th and 6th postoperative weeks, while at 2 weeks of observation, there was no significant difference among the control, A-PRF and ZnO-NP groups; however, there was a significant difference between the three groups and the MV group. At the end of the observation period (at six weeks), the highest ultrasonographic score was obtained in the MV and ZnO-NP groups (4).

**DISCUSSION**

Animal models are crucial to the understanding of tendinopathies and Achilles tendon ruptures in terms of surgery and recovery.(BEASON et al.,

2012; YASUDA et al., 2000). Because the rabbit is readily available, manageable, and has a suitable-sized Achilles tendon, it has been utilized to investigate the tendon. (JASSEM et al.,

2001; THERMANN et al., 2001). Moreover, the Achilles tendon of rabbits is located superficially and somewhat large, and this approach is practical and economic (DE CESAR NETTO et al., 2018; SKALEC et al., 2016). Regarding clinical signs, the operated rabbits in the different groups had good general health conditions at the first clinical investigation, and there was no significant difference between the groups. This might be due to the proper postoperative care, which led to the control of infection; these results agree with those reported by Bennett et al. and Atkins et al. (ATKINS, 1960; BENNETT JR and BEESON, 1953). In parallel, lameness scores, as assessed by a blind observer, provide a functional dimension to our evaluation (DUNTHORN et al., 2015). By tracking the animals' movement patterns and assessing pain levels, we gained insights into the practical implications of the healing process (MARTIN et al., 2018). This dual evaluation strategy, in which ultrasonography and lameness scores are combined, offers a holistic perspective on tendon recovery, bridging the gap between structural improvements and functional outcomes. By the second week following implantation, every rabbit that had surgery had become lame, experienced pain when moving the operated hind limb, and experienced difficulty fully flexing the tarsal joint. These symptoms could have been brought on by the surgical procedure, which involved skin incisions and tendon cutting, as well as the relatively lengthy period of immobilization and exercise restriction that followed the surgery.; these findings agreed with Stoll et al. (STOLL et al., 2011). Nevertheless, these symptoms vanished after four weeks in the ZnO-NP-treated group and six weeks in the MV-treated group, which is consistent

with the anti-inflammatory and antibacterial characteristics of these treatment groups. (LO SICCO et al., 2017; WANG et al., 2023). All groups showed evidence of tendon adhesion to skin at the two-week mark following implantation; however, in the control group, this adhesion was more severe than in the other groups. In the treatment groups, adhesion gradually diminished until the tendon was slidable at the six-week mark following implantation. Since these exogenous cells predominate over endogenous tenocytes, the surrounding tissues attach to the repair area and form adhesions that limit the tendinous gliding capacity and, consequently, the range of motion. This adhesion can be explained by the invasion of the repair site by granulation tissue and tenocytes from the surrounding tissue following disruption of the synovial sheath during injury or surgery (SHARMA and MAFFULLI, 2006; ZHOU and LU, 2021). In this study, the adhesion of the treated tendons improved faster than that of the control tendons. APRF, MVs, and ZnO-NPs were used; they may have reduced acute inflammation and postsurgical oedema. They also prevented the formation of peritendinous adhesions and produced painless mobility; these data are consistent with those of Naderi et al. (NADERI et al., 2018). Ultrasound is a noninvasive and dynamic tool for assessing Achilles tendon regeneration (S.-Y. LEE et al., 2017). It is available, relatively inexpensive, repeatable, and can be performed anywhere (L. LEE and DECARA, 2020). Ultrasonography enables the assessment of tendon regeneration and dimensions and correlation of the 3 phases of tendon healing: inflammatory, proliferative, and remodeling (AGARWAL et al., 2012; KLAUSER et al., 2014). Several previous studies have demonstrated the

use of ultrasound for evaluating tendon health, and they were designed to determine the correlation between measured ultrasound properties and tissue properties (DUENWALD-KUEHL et al., 2012; KULIG et al., 2013, 2016). In this study, we used longitudinal sonographically sections because the cross-sectional area was not diagnostic due to the narrow diameter of the rabbit's tendon, while the longitudinal sections were suitable and considered diagnostic (BUSCHMANN et al., 2014). A normal tendon structure is observed ultrasonographical in the form of linear echoes representing acoustic borders between collagen fibers and loose connective tissue permeating the fascicles (NEUHOLD et al., 1992); while during the healing process after Achilles tendon injury, the collagen fibrils are arranged parallel to the longitudinal axis of the tendon (KOMATSU et al., 2016). The ultrasound findings in this study can be correlated with tendon healing phases in humans and rabbits (KOMATSU et al., 2016; THERMANN et al., 2002). During the remodeling phase, fibroblasts produce, deposit, orient, and cross-link fibrillar collagen (THOMOPOULOS et al., 2015). The fibrillar morphology in the US is gradual, as fibrillar collagen is cross-linked and aligns along the long axis of the repaired tendon (THOMOPOULOS et al., 2015). In the present study, the repaired tendons mostly exhibited a normal fibrillar pattern that appeared faster in both the MV- and ZnO-NP-treated groups at the 6<sup>th</sup> week than in the control group (HIRAMATSU et al., 2018; MERSMANN et al., 2019). Tendon margins have been described in the healthy Achilles tendon as thin lines surrounding the Achilles tendon and as regular isoechoic or slightly hyperechoic; however, in pathological

situations, the para-tendon shows irregularities of the tendon margins, fluid collection (hypoechoic), and adhesions between the para-tendon and peritendinous tissues due to inflammatory phenomena and increased thickness (LEUNG and GRIFFITH, 2008; ZABRZYŃSKI et al., 2018). The current study revealed alterations in the tendon margins (para-tendons), and normal tendon margins appeared faster in both the MV- and ZnO-NP-treated groups at the 6<sup>th</sup> week than in the control group. These data agreed with those of *Leung and Griffith et al.* (LEUNG and GRIFFITH, 2008). Presence of a hypoechoic area in the mid-section of the Achilles tendon in our study at the 2nd week post implantation in all groups. This can be explained by the presence of hemorrhage, fibrinolysis, PRF membrane formation, MV gel formation and early granulation tissue formation (KULIG et al., 2013). The increase in the incidence of hyperechoic areas along the tendon fibrils of the Achilles tendon in the current study at 2 weeks after surgery in the control and A-PRF-treated groups and in the MV- and ZnO-NP-treated groups at 4 weeks may be attributed to the occurrence of intra-tendinous scar formation. These results are consistent with those of *Niki et al.* and *Ehrle et al.* (EHRLE et al., 2021; NIKI et al., 2013) who reported that intra-tendinous scar formation resulted in multiple hyperechoic areas.

## CONCLUSIONS

At the end of the study, ultrasonographic locomotive observation revealed the superiority of the MV and ZnO-NP groups for the treatment of Achilles tendon defects compared with the A-PRF and control groups when used to fill a tendon defect in a rabbit model.

## REFERENCES

- ABD-ELKAWI, M., SHARSHAR, A., MISK, T., ELGOHARY, I., GADALLAH, S. (2023): Effect of calcium carbonate nanoparticles, silver nanoparticles and advanced platelet-rich fibrin for enhancing bone healing in a rabbit model. *Scientific Reports*, 13(1), 15232. DOI: 10.1038/s41598-023-42292-x
- AGARWAL, A., QURESHI, N. A., KUMAR, P., GARG, A., GUPTA, N. (2012): Ultrasonographic evaluation of Achilles tendons in clubfeet before and after percutaneous tenotomy. *Journal of Orthopaedic Surgery*, 20(1), 71–74. DOI: 10.1177/230949901202000114
- AL-HUSSEIN, S. S. A., AL-DIRAWI, A. A. I., AL-KHALIFAH, R. M. N. (2023): Histopathological Study of the Effect of Xenogeneic Platelet-Rich Fibrin on Achilles Tendon Healing in Rabbit. *Bionatura*, 8(2), 1–10. <https://doi.org/10.21931/RB/CSS/2023.08.02.24>
- ALKETBI, T. (2016): *Effect of isometric training with short or long rest periods on Achilles tendon morphology: an ultrasound tissue characterization study*. University of British Columbia. <http://hdl.handle.net/2429/59958> DOI:10.14288/1.0340306
- ATKINS, E. (1960): Pathogenesis of fever. *Physiological Reviews*, 40(3), 580–646. <https://doi.org/10.1152/physrev.1960.40.3.580>
- BEASON, D. P., KUNTZ, A. F., HSU, J. E., MILLER, K. S., SOSLOWSKY, L. J. (2012): Development and evaluation of multiple tendon injury models in the mouse. *Journal of Biomechanics*, 45(8), 1550–1553. <https://doi.org/10.1016/j.jbiomech.2012.02.022>
- BECHERI, A., DÜRR, M., LO NOSTRO, P., BAGLIONI, P. (2008): Synthesis and characterization of zinc oxide nanoparticles: application to textiles as UV-absorbers. *Journal of Nanoparticle Research*, 10, 679–689. <https://doi.org/10.1007/s11051-007-9318-3>
- BENNETT JR, I. L., BEESON, P. B. (1953): Studies on the pathogenesis of fever: II. Characterization of fever-producing substances from polymorphonuclear leukocytes and from the fluid of sterile exudates. *The Journal of Experimental Medicine*, 98(5), 493. doi: [10.1084/jem.98.5.493](https://doi.org/10.1084/jem.98.5.493)
- BUSCHMANN, J., PUIPPE, G., BÜRGISSER, G. M., BONAVOGLIA, E., GIOVANOLI, P., CALCAGNI, M. (2014): Correspondence of high-frequency ultrasound and histomorphometry of healing rabbit Achilles tendon tissue. *Connective Tissue Research*, 55(2), 123–131. <https://doi.org/10.3109/03008207.2013.870162>
- COCUCCI, E., MELDOLESI, J. (2015): Ectosomes and exosomes: shedding the confusion between extracellular vesicles. *Trends in Cell Biology*, 25(6), 364–372. DOI:<https://doi.org/10.1016/j.tcb.2015.01.004>
- CONZEMIUS, M. G., BROWN, T. D., ZHANG, Y., ROBINSON, R. A. (2002): A new animal model of

- femoral head osteonecrosis: one that progresses to human-like mechanical failure. *Journal of Orthopaedic Research*, 20(2), 303–309.  
[https://doi.org/10.1016/S0736-0266\(01\)00108-5](https://doi.org/10.1016/S0736-0266(01)00108-5)
- DE CESAR NETTO, C., GODOY-SANTOS, A. L., PONTIN, P. A., NATALINO, R. J. M., PEREIRA, C. A. M., DE OLIVEIRA LIMA, F. D., DA FONSECA, L. F., STAGGERS, J. R., CAVINATTO, L. M., SCHON, L. C., DE CAMARGO, O. P., FERNANDES, T. D. (2018): Novel animal model for Achilles tendinopathy: Controlled experimental study of serial injections of collagenase in rabbits. *PLoS ONE*, 13(2).  
<https://doi.org/10.1371/journal.pone.0192769>
- DUENWALD-KUEHL, S., LAKES, R., VANDERBY JR, R. (2012): Strain-induced damage reduces echo intensity changes in tendon during loading. *Journal of Biomechanics*, 45(9), 1607–1611.  
<https://doi.org/10.1016/j.jbiomech.2012.04.004>
- DUNTHORN, J., DYER, R. M., NEERCHAL, N. K., MCHENRY, J. S., RAJKONDAWAR, P. G., STEINGRABER, G., TASCH, U. (2015): Predictive models of lameness in dairy cows achieve high sensitivity and specificity with force measurements in three dimensions. *Journal of Dairy Research*, 82(4), 391–399. DOI:  
<https://doi.org/10.1017/S002202991500028X>
- EHRLE, A., LILGE, S., CLEGG, P. D., MADDOX, T. W. (2021): Equine flexor tendon imaging part 1: Recent developments in ultrasonography, with focus on the superficial digital flexor tendon. *The Veterinary Journal*, 278, 105764.  
<https://doi.org/10.1016/j.tvjl.2021.105764>
- EL-SHAER, H., ELWAKIL, B. H., BAKR, B. A., ELDRIENY, A. M., EL-KHATIB, M., CHONG, K. P., ABO GAZIA, A. A. (2022): Physiotherapeutic Protocol and ZnO Nanoparticles: A Combined Novel Treatment Program against Bacterial Pyomyositis. In *Biology* (Vol. 11, Issue 10).  
<https://doi.org/10.3390/biology11101393>
- EL-TOOKHY, O. S., SHAMAA, A. A., SHEHAB, G. G., ABDALLAH, A. N., AZZAM, O. M. (2017): Histological evaluation of experimentally induced critical size defect skin wounds using exosomal solution of mesenchymal stem cells derived microvesicles. *International Journal of Stem Cells*, 10(2), 144–153. doi: 10.15283/ijsc17043
- GRECU, A. F., RECLARU, L., ARDELEAN, L. C., NICA, O., CIUCĂ, E. M., CIUREA, M. E. (2019): Platelet-rich fibrin and its emerging therapeutic benefits for musculoskeletal injury treatment. *Medicina*, 55(5), 141.  
<https://doi.org/10.3390/medicina55050141>
- HIRAMATSU, K., TSUJII, A., NAKAMURA, N., MITSUOKA, T. (2018): Ultrasonographic evaluation of the early healing process after achilles tendon repair. *Orthopaedic Journal of Sports Medicine*, 6(8), 2325967118789883.  
<https://doi.org/10.1177/2325967118789883>

- HOLMES, G. B., LIN, J. (2006): Etiologic factors associated with symptomatic achilles tendinopathy. *Foot and Ankle International*, 27(11), 952–959. <https://doi.org/10.1177/107110070602701115>
- JASSEM, M., ROSE, A. T., MEISTER, K., INDELICATO, P. A., WHEELER, D. (2001). Biomechanical analysis of the effect of varying suture pitch in tendon graft fixation. *The American Journal of Sports Medicine*, 29(6), 734–737. <https://doi.org/10.1177/03635465010290061>
- KARIMI, K., and ROCKWELL, H. (2019): The benefits of platelet-rich fibrin. *Facial Plastic Surgery Clinics*, 27(3), 331–340. DOI:<https://doi.org/10.1016/j.fsc.2019.03.005>
- KHALIL, A. M., EL-KHATIB, A. M., EL-KHATIB, M. (2019): Synthesis of hexagonal nanozinc by arc discharge for antibacterial water treatment. *Surface Innovations*, 8(3), 165–171. <https://doi.org/10.1680/jsuin.19.00050>
- KIM, S. B., KWON, D. R., KWAK, H., SHIN, Y. B., HAN, H., LEE, J. H., CHOI, S. H. (2010): Additive effects of intra-articular injection of growth hormone and hyaluronic acid in rabbit model of collagenase-induced osteoarthritis. *Journal of Korean Medical Science*, 25(5), 776–780. doi: 10.3346/jkms.2010.25.5.776
- KLAUSER, A. S., MIYAMOTO, H., BELLMANN-WEILER, R., FEUCHTNER, G. M., WICK, M. C., JASCHKE, W. R. (2014): Sonoelastography: musculoskeletal applications. *Radiology*, 272(3), 622–633. <https://doi.org/10.1148/radiol.14121765>
- KOMATSU, I., WANG, J. H. C., IWASAKI, K., SHIMIZU, T., OKANO, T. (2016): The effect of tendon stem/progenitor cell (TSC) sheet on the early tendon healing in a rat Achilles tendon injury model. *Acta Biomaterialia*, 42, 136–146. <https://doi.org/10.1016/j.actbio.2016.06.026>
- KULIG, K., CHANG, Y.-J., WINIARSKI, S., BASHFORD, G. R. (2016): Ultrasound-based tendon micromorphology predicts mechanical characteristics of degenerated tendons. *Ultrasound in Medicine and Biology*, 42(3), 664–673. <https://doi.org/10.1016/j.ultrasmedbio.2015.11.013>
- KULIG, K., LANDEL, R., CHANG, Y., HANNANVASH, N., REISCHL, S. F., SONG, P., BASHFORD, G. R. (2013): Patellar tendon morphology in volleyball athletes with and without patellar tendinopathy. *Scandinavian Journal of Medicine and Science in Sports*, 23(2), e81–e88. <https://doi.org/10.1111/sms.12021>
- LEE, L., DECARA, J. M. (2020): Point-of-care ultrasound. *Current Cardiology Reports*, 22, 1–10. <https://doi.org/10.1007/s11886-020-01394-y>
- LEE, S.-Y., CHIEH, H.-F., LIN, C.-J., JOU, I.-M., SUN, Y.-N., KUO, L.-C., WU, P.-T., SU, F.-C. (2017). Characteristics of Sonography in a Rat Achilles Tendinopathy Model: Possible Non-invasive Predictors of Biomechanics. *Scientific Reports*,

- 7(1), 5100.  
<https://doi.org/10.1038/s41598-017-05466-y>
- LEUNG, J. L. Y., GRIFFITH, J. F. (2008): Sonography of chronic Achilles tendinopathy: a case-control study. *Journal of Clinical Ultrasound*, 36(1), 27–32.  
<https://doi.org/10.1002/jcu.20388>
- LO SICCO, C., REVERBERI, D., BALBI, C., ULIVI, V., PRINCIPI, E., PASCUCCI, L., BECHERINI, P., BOSCO, M. C., VAREGIO, L., FRANZIN, C. (2017): Mesenchymal stem cell-derived extracellular vesicles as mediators of anti-inflammatory effects: endorsement of macrophage polarization. *Stem Cells Translational Medicine*, 6(3), 1018–1028.  
<https://doi.org/10.1002/sctm.16-0363>
- MARTIN, J. A., BRANDON, S. C. E., KEULER, E. M., HERMUS, J. R., EHLERS, A. C., SEGALMAN, D. J., ALLEN, M. S., THELEN, D. G. (2018): Gauging force by tapping tendons. *Nature Communications*, 9(1), 1592.  
<https://doi.org/10.1038/s41467-018-03797-6>
- MERSMANN, F., PENTIDIS, N., TSAI, M.-S., SCHROLL, A., ARAMPATZIS, A. (2019): Patellar tendon strain associates to tendon structural abnormalities in adolescent athletes. *Frontiers in Physiology*, 10, 963.  
<https://doi.org/10.3389/fphys.2019.00963>
- MOHAMMADI, M. R., RIAZIFAR, M., PONE, E. J., YERI, A., VAN KEUREN-JENSEN, K., LÄSSER, C., LOTVALL, J., ZHAO, W. (2020): Isolation and characterization of microvesicles from mesenchymal stem cells. *Methods*, 177, 50–57.  
<https://doi.org/https://doi.org/10.1016/j.jymeth.2019.10.010>
- NADERI, N., KARPONIS, D., MOSAHEBI, A., SEIFALIAN, A. M. (2018): Nanoparticles in wound healing; from hope to promise, from promise to routine. *Frontiers in Bioscience-Landmark*, 23(6), 1038–1059.  
<https://doi.org/10.2741/4632>
- NEUHOLD, A., STISKAL, M., KAINBERGER, F., SCHWAIGHOFER, B. (1992): Degenerative Achilles tendon disease: assessment by magnetic resonance and ultrasonography. *European Journal of Radiology*, 14(3), 213–220.  
[https://doi.org/10.1016/0720-048X\(92\)90090-V](https://doi.org/10.1016/0720-048X(92)90090-V)
- NIKI, H., NAKAJIMA, H., HIRANO, T., OKADA, H., BEPPU, M. (2013): Ultrasonographic observation of the healing process in the gap after a Ponseti-type Achilles tenotomy for idiopathic congenital clubfoot at two-year follow-up. *Journal of Orthopaedic Science*, 18, 70–75.  
<https://doi.org/10.1007/s00776-012-0312-y>
- PANT, S., HILTON, H., BURCZYNSKI, M. E. (2012): The multifaceted exosome: biogenesis, role in normal and aberrant cellular function, and frontiers for pharmacological and biomarker opportunities. *Biochemical Pharmacology*, 83(11), 1484–1494.  
<https://doi.org/10.1016/j.bcp.2011.12.037>
- SAINI, K., DEWAL, M. L., ROHIT, M. (2010): Ultrasound imaging

- and image segmentation in the area of ultrasound: a review. *International Journal of Advanced Science and Technology*, 24. <https://api.semanticscholar.org/CorpusID:14579436>
- SHARMA, P., MAFFULLI, N. (2006): Biology of tendon injury: healing, modeling and remodeling. *Journal of Musculoskeletal and Neuronal Interactions*, 6(2), 181. <https://api.semanticscholar.org/CorpusID:6334881>.
- SHOJAEE, A., PARHAM, A. (2019): Strategies of tenogenic differentiation of equine stem cells for tendon repair: current status and challenges. *Stem Cell Research and Therapy*, 10(1), 1–13. <https://doi.org/10.1186/s13287-019-1291-0>
- SINGH, T. A., SHARMA, A., TEJWAN, N., GHOSH, N., DAS, J., SIL, P. C. (2021): A state of the art review on the synthesis, antibacterial, antioxidant, antidiabetic and tissue regeneration activities of zinc oxide nanoparticles. *Advances in Colloid and Interface Science*, 295, 102495. <https://doi.org/10.1016/j.cis.2021.102495>
- SKALEC, A., JANECEK, M., JANUS, I., CHRÓSZCZ, A., HENKLEWSKI, R. (2016): Rabbit common calcanean tendon as an animal model: ultrasonographic anatomy and morphometry. *Folia Morphologica*, 75(1), 93–100. DOI: 10.5603/FM.a2015.0071
- SODE, J., OBEL, N., HALLAS, J., LASSEN, A. (2007): Use of fluroquinolone and risk of Achilles tendon rupture: a population-based cohort study. *European Journal of Clinical Pharmacology*, 63, 499–503. <https://doi.org/10.1007/s00228-007-0265-9>
- STEINMANN, S., PFEIFER, C. G., BROCHHAUSEN, C., DOCHEVA, D. (2020): Spectrum of tendon pathologies: Triggers, trails and end-state. *International Journal of Molecular Sciences*, 21(3), 844. <https://doi.org/10.3390/ijms21030844>
- STOLL, C., JOHN, T., CONRAD, C., LOHAN, A., HONDKE, S., ERTEL, W., KAPS, C., ENDRES, M., SITTINGER, M., RINGE, J. (2011): Healing parameters in a rabbit partial tendon defect following tenocyte/biomaterial implantation. *Biomaterials*, 32(21), 4806–4815. <https://doi.org/10.1016/j.biomaterials.2011.03.026>
- THERMANN, H., FRERICHS, O., BIEWENER, A., KRETTEK, C. (2001): Healing of the Achilles tendon: an experimental study. *Foot and Ankle International*, 22(6), 478–483. <https://doi.org/10.1177/107110070102200604>
- THERMANN, H., FRERICHS, O., HOLCH, M., BIEWENER, A. (2002): Healing of Achilles tendon, an experimental study: part 2—histological, immunohistological and ultrasonographic analysis. *Foot and Ankle International*, 23(7), 606–613. <https://doi.org/10.1177/107110070202300704>
- THOMOPOULOS, S., PARKS, W. C., RIFKIN, D. B., DERWIN, K. A.

- (2015): Mechanisms of tendon injury and repair. *Journal of Orthopaedic Research*, 33(6), 832–839.  
<https://doi.org/10.1002/jor.22806>
- TSENG, T.-C., HSU, S. (2014): Substrate-mediated nanoparticle/gene delivery to MSC spheroids and their applications in peripheral nerve regeneration. *Biomaterials*, 35(9), 2630–2641.  
<https://doi.org/10.1016/j.biomaterials.2013.12.021>
- WANG, W., LIU, M., SHAFIQ, M., LI, H., HASHIM, R., MOHAMED, E.-N., HANY, E.-H., MORSI, Y., MO, X. (2023): Synthesis of oxidized sodium alginate and its electrospun bio-hybrids with zinc oxide nanoparticles to promote wound healing. *International Journal of Biological Macromolecules*, 232, 123480.  
<https://doi.org/10.1016/j.ijbiomac.2023.123480>
- XIE, L., MAO, M., ZHOU, L., JIANG, B. (2016): Spheroid mesenchymal stem cells and mesenchymal stem cell-derived microvesicles: two potential therapeutic strategies. *Stem Cells and Development*, 25(3), 203–213.  
<https://doi.org/10.1089/scd.2015.0278>
- 278
- YASUDA, T., KINOSHITA, M., ABE, M., SHIBAYAMA, Y. (2000): Unfavorable effect of knee immobilization on Achilles tendon healing in rabbits. *Acta Orthopaedica Scandinavica*, 71(1), 69–73.  
<https://doi.org/10.1080/00016470052943937>
- ZABRZYŃSKI, J., ZABRZYŃSKA, A., GRZANKA, D. (2018): Tendon—function-related structure, simple healing process and mysterious ageing. *Folia Morphologica*, 77(3), 416–427.  
DOI: 10.5603/FM.a2018.0006
- ZALAMA, E., KARROUF, G., RIZK, A., SALAMA, B., SAMY, A. (2022): Does zinc oxide nanoparticles potentiate the regenerative effect of platelet-rich fibrin in healing of critical bone defect in rabbits? *BMC Veterinary Research*, 18(1), 130.  
<https://doi.org/10.1186/s12917-022-03231-6>
- ZHOU, H., LU, H. (2021): Advances in the development of anti-adhesive biomaterials for tendon repair treatment. *Tissue Engineering and Regenerative Medicine*, 18, 1–14.  
<https://doi.org/10.1007/s13770-020-00300-5>